JOURNAL OF THE KOREAN ASTRONOMICAL SOCIETY
31: 39 ~ 50, 1998

UBV CCD PHOTOMETRY OF THE OPEN CLUSTER BERKELEY 2

ANN, HONG BAE, PARK, YOON HO AND KANG, YONG WOO
Department of Earth Sciences, Pusan National University, Pusan 609-735, Korea
hbann@astrophys.es.pusan.ac.kr
(Received Mar. 16, 1998; Accepted Apr. 6, 1998)

ABSTRACT

We present *UBV* CCD photometry of Be 2, previously unstudied open cluster. Our photometry covers a field of $3'.2 \times 3'.8$ of the sky centered on the cluster, which is slightly smaller than the cluster diameter estimated to be about $260''$. We have determined the reddening, distance, age and metallicity of the cluster by fitting the Padova isochrones to the observed stellar distributions in color-magnitude diagram as well as main sequence fitting: $E(B-V) = 0.8 \pm 0.05$, $(m-M)_o = 13.6 \pm 0.1, log(t) = 8.9 \pm 0.1$, and Z =0.008. The present photometry shows that Be 2 is a distant open cluster of intermediate age. that it is a distant intermediate-age open cluster.

Key Words : open clusters: individual (Be 2), C-M diagram, age, distance

I. INTRODUCTION

A study of open clusters provides us much information about various astrophysical phenomena. Young open clusters seem to be one of the best tools for our understanding of the star formation process. Probing intermediate-age and old open clusters makes it possible to decipher the early evolutionary histoty of the galactic disk. Moreover, color-magnitude diagrams (CMDs) of open clusters provide critical constraints on the stellar evolution models.

Since the advent of CCDs in astronomy, many efforts have been made to obtain accurate CMDs and color-color diagrams of open clusters to extend our understanding of the galactic disk (Phelps, Janes & Montgomery 1994; Phelps & Janes 1994; Kaluzny 1994). However, most of the recent efforts have focused their attention primarily on the observations of rich clusters of which distances and ages are known from the previous studies based on photoelectric or photographic photometry. Moreover, if we consider that more than half of the known open clusters are classified as Trumpler class p and m (Lyngå 1987), it is desirable to study these clusters as well as rich ones.

Be 2 is a poorly known open cluster which is located between β Cas and χ Cas ($\alpha_{1950} = 05:30:24, \delta_{1950} = +00°11'; l = 203.°50, b = -17.°28$). It is classified as Trumpler class IIp in the Catalogue of Open Cluster Data (COCD, Lyngå 1987), with an angular diameter of $2'$. The present observations have been conducted as a part of our ongoing program which aims to observe poorly studied or unstudied open clusters in order to enlarge our understanding of the cluster itself and the Galaxy as a whole.

In this paper we present *UBV* CCD photometry of Be 2, which, to the best of our knowledge, has been neglected in previous photometric studies. The primary goal of our photometry is to determine the distance and age of Be 2 using the observed CMD and theoretical isochrones. In section 2, we present the observations and data reduction, and the results of the present study are given in section 3. Brief discussions on the physical parameters of Be 2 derived from the present photometry are given in section 4, and the summary of the present study is given in the last section.

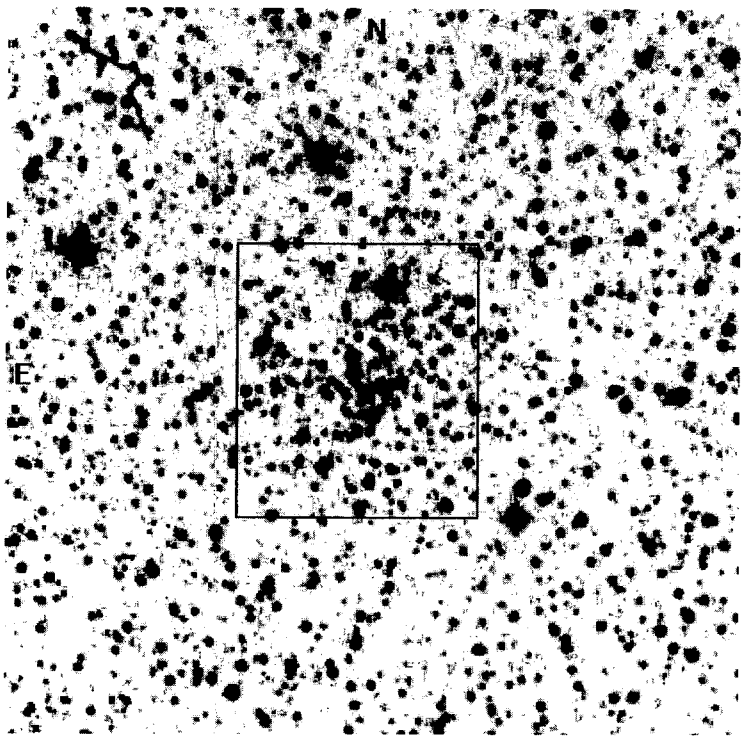

Fig. 1. Identificaton map for the imaged region of Be 2, reproduced from the Digitized Sky Survey, DSS. Location of the CCD image is indicated by a rectangle (3.′2 × 3.′8). North is up and east is to the left.

II. OBSERVATIONS AND DATA REDUCTION

The observations in *UBV* Johnson pass bands were carried out for a field of Be 2, with Photometrics 512 × 512 CCD which was attached to the cassegrain focus of the 61cm telescope at the Sobaeksan Observatory, Korea, on two nights of 1997 November 1-2. The pixel size is 20 μm which corresponds to 0.″5 on the sky. Readout noise of the system is about $8e^{-1}$ and the gain is $9e^{-1}$/ADU. Bias and dark frames were obtained several times during the nights and the flat-field exposures were made on the twilight sky. For the calibration purposes, the standard stars in NGC 7790 (Sandage 1955; Christian *et al.* 1985) were observed. We observed the standard stars several times to monitor the variation of the sky condition during the nights. To avoid image drift due to poor tracking of the telescope, the observations of the cluster and the standard stars were made using multiple exposure times of 100 s in duration. Fig. 1 shows the identification map of Be 2 reproduced from Digitized Sky Survey (DSS). The size of the field is 10′ × 10′ and the area covered by our observation is indicated by a rectangle. North is up and east is to the left in Fig. 1. The seeing during the observation was between 2.0 and 2.5 arcsec FWHM. The journal of the observations is given in Table 1.

Table 1. Journal of observations

Date (UT)	Filter	Exposure Time (secs × number)	Seeing (arcsec)
Nov. 1	V	100 × 14	2.0
	B	100 × 32	2.2
	U	100 × 62	2.5
Nov. 2	V	100 × 17	2.1
	B	100 × 32	2.2
	U	100 × 76	2.5

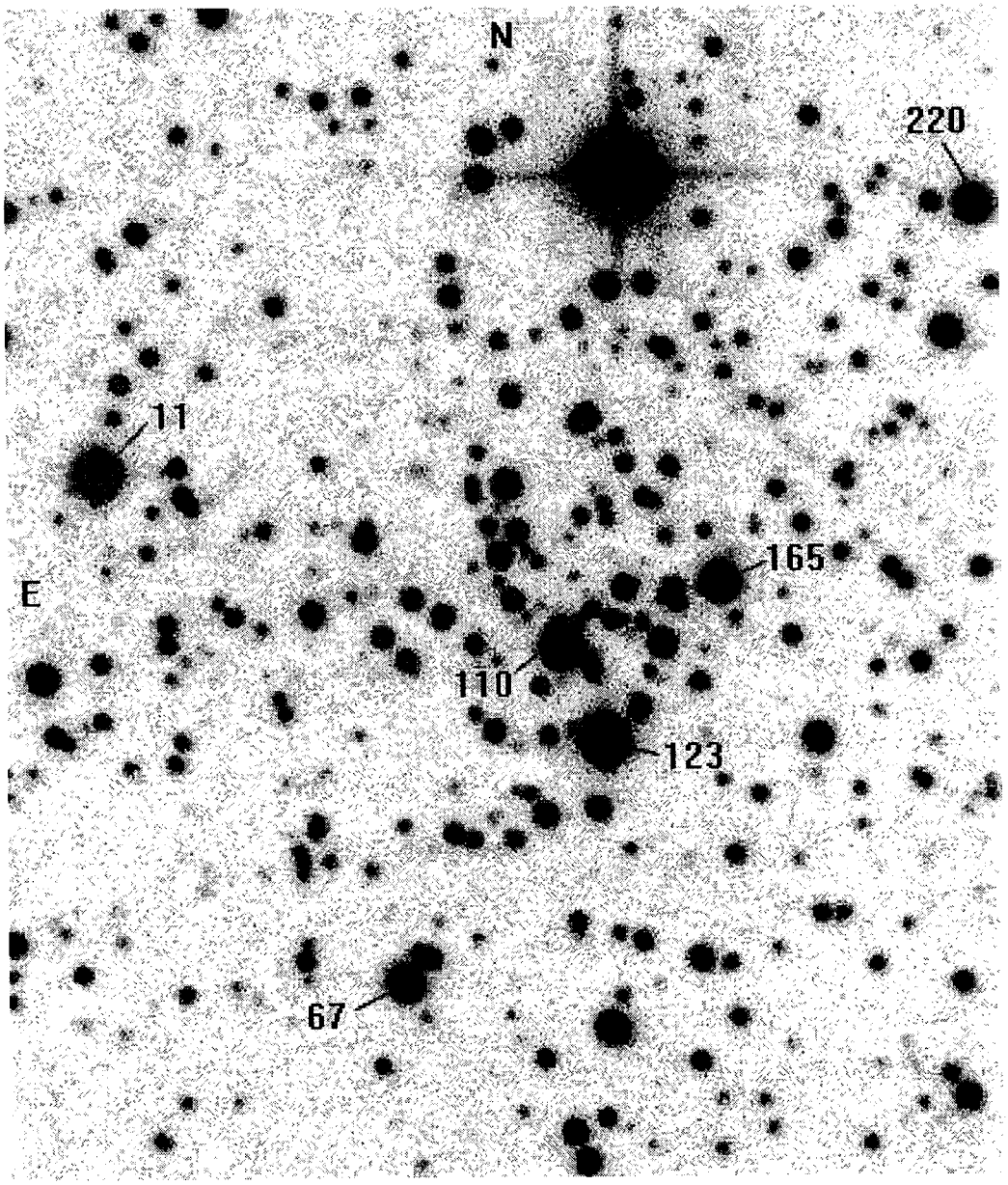

Fig. 2. *V*-band image resulted from the combination of 31 flat-fielded frames. Six bright stars from Table 2 are identified. The image sige is $3'.2 \times 3'.8$ and the orientation is the same as that of Fig 1.

The basic CCD reduction was carried out using the CCDRED package within IRAF. This procedure involved the subtraction of the mean bias frame with overscan correction, subtraction of dark frame, trimming of the data section, and flat-fielding. The flat-field frames were prepared by combining all the flat-field frames obtained during the observing run for each filter. All the good frames were combined to make a deep image for each filter. Fig. 2 shows the *V*-band image resulted from the combination of 31 flat-fielded frames. The size of the image is $3.'2 \times 3.'8$ and the orientation is the same as that of Fig 1. The magnitude estimate of the stars on the combined images was made by using DAOPHOT package in IRAF and the magnitudes of the standard stars were estimated by using aperture photometry.

Because we measured magnitudes of stars from the images which were made by combining several tens of frames with different air masses, the transformation of the instrumental magnitudes to the standard system was made by two steps. First, we determined magnitudes of 17 local standard stars, located in the cluster region, in the standard

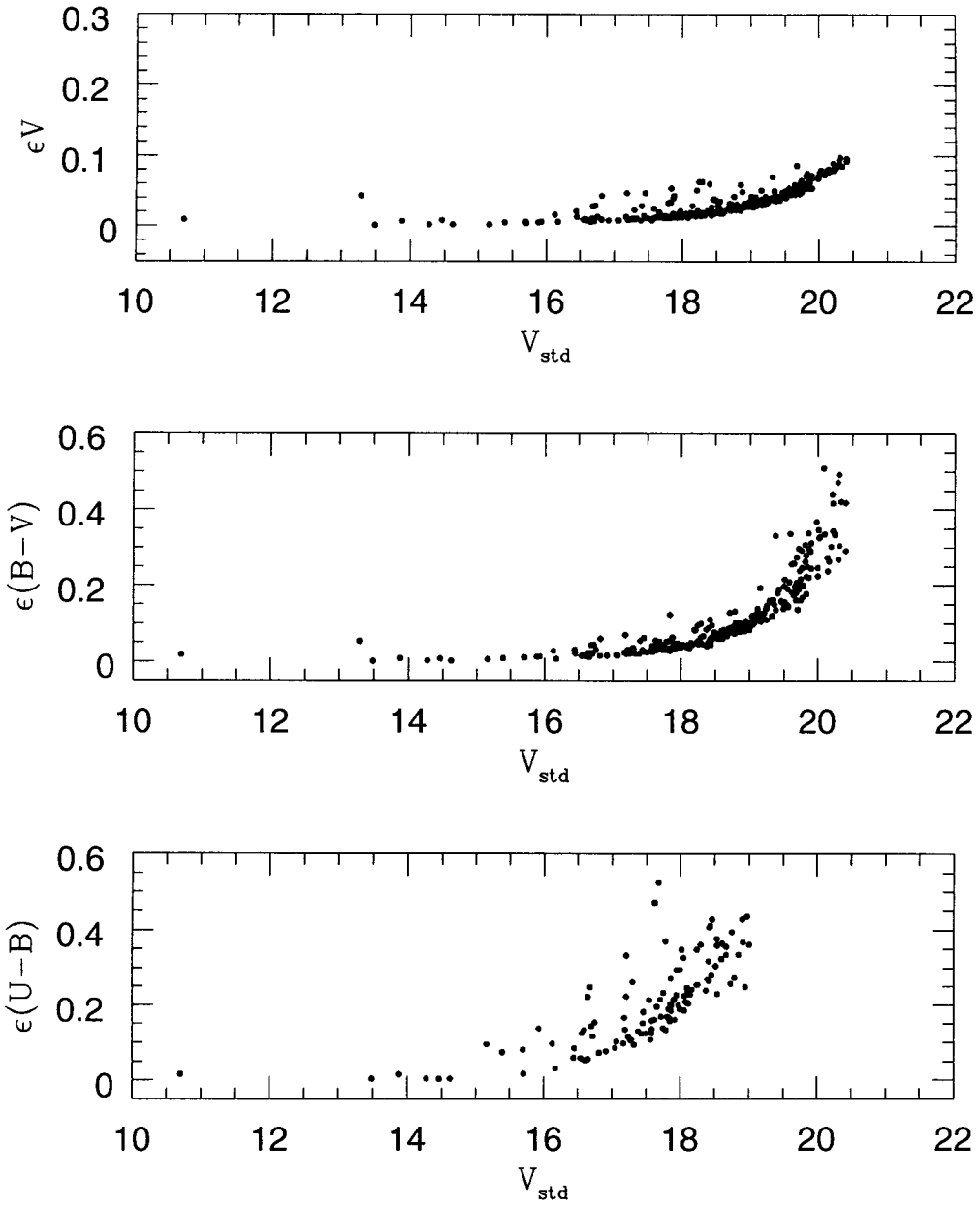

Fig. 3. The photometric errors from DAOPHOT as a function of V magnitude.

system using the following transformation equations

$$V = v - 5.901(\pm 0.026) - 0.146(\pm 0.018)X + 0.008(\pm 0.064)(B - V)$$

$$B = b - 6.662(\pm 0.037) - 0.217(\pm 0.025)X + 0.186(\pm 0.084)(B - V)$$

$$U = u - 7.860(\pm 0.036) - 0.549(\pm 0.024)X + 0.229(\pm 0.240)(U - B)$$

where the capital letters stand for the magnitudes in the standard system, the lower case letters for the instrumental magnitudes, and X for the airmass. The coefficients were determined by a least-squares fit of the instrumental magnitudes of the standard stars in NGC 7790 to the magnitudes in the standard system (Sandage 1955; Christen *et al.* 1985). Then, we transformed the instrumental magnitudes of the stars estimated from the deep images, by the following equations derived from the magnitudes of the local standard stars,

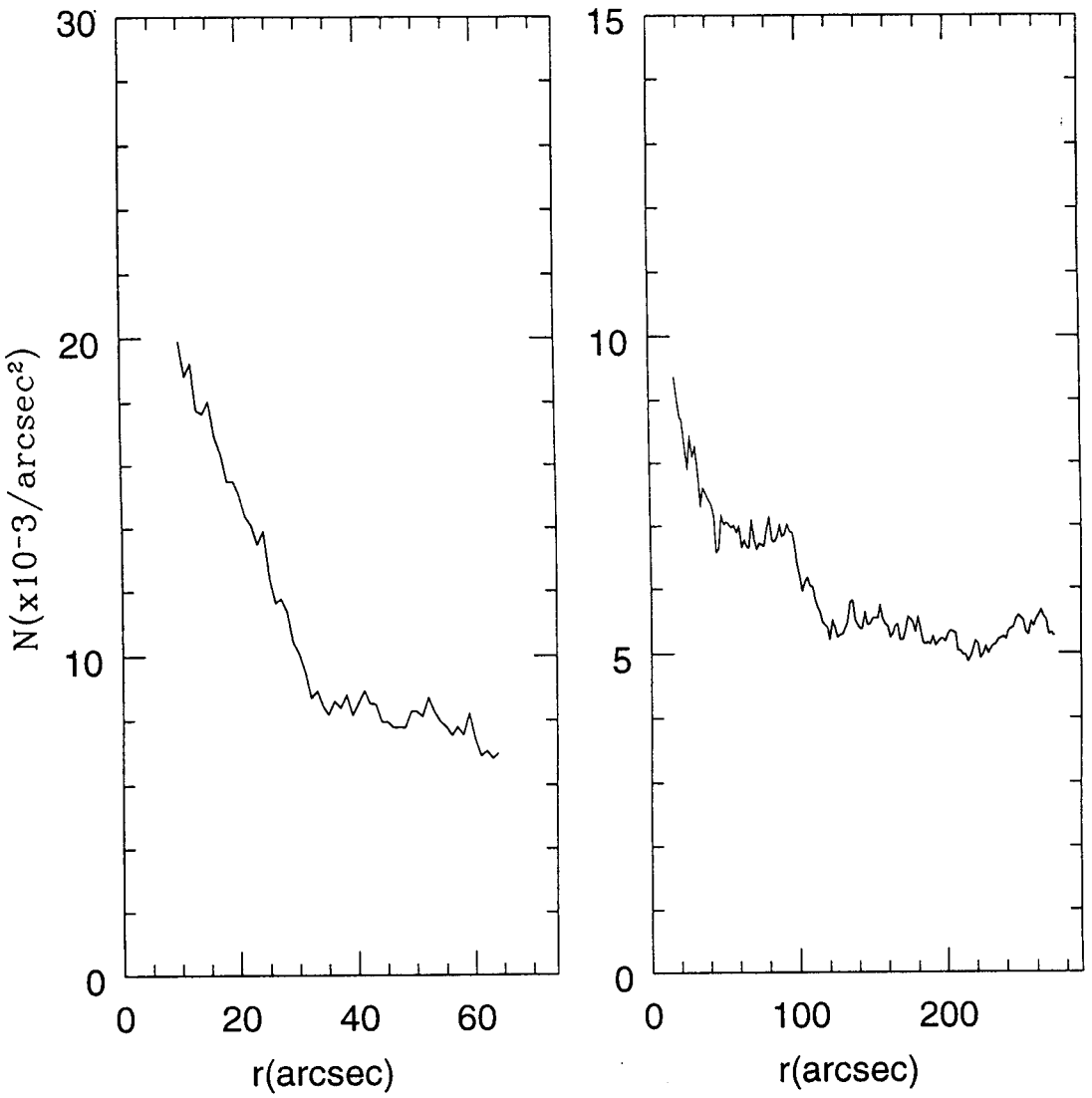

Fig. 4. Radial surface density profiles of Be 2. The left panel shows the density distribution from the CCD image and the right panel is that for the DSS image.

$$V = v - 6.102(\pm 0.013) + 0.003(\pm 0.010)(B - V)$$

$$B = b - 6.917(\pm 0.013) + 0.167(\pm 0.010)(B - V)$$

$$U = u - 8.446(\pm 0.028) + 0.206(\pm 0.036)(U - B)$$

where the capital letters stand for the magnitudes in the standard system and the lower case letters for the instrumental magnitudes.

Fig. 3 shows the photometric errors in colors calculated by ALLSTAR. The errors in colors are larger than 0.1 for the stars with $V > 18$ in *(B-V)* colors and $V > 17$ in *(U-B)* colors, respectively. In Table 2 we present the magnitudes and colors of all the stars in our combined images which are brighter than $V \sim 19.4$ except for the brightest star that is saturated on the CCD frames. Column 1 gives the identification number and the column 2 and 3 represent the x and y coordinates in pixel units of which the origin is the lower left corner of the CCD image given in Fig. 2. The magnitude and colors are given in the remaining columns.

We followed the procedures outlined by Massey & Davis(1992) for the stellar photometry using PSF. The detection of the stellar images was performed with the FIND routines and the aperture photomery for the detected stars was made by PHOTOMERTY. The final instrumental magnitudes were measured by PSF fitting using ALLSTAR. Two or three passes of ALLSTAR were enough to detect the faintest stars in the combined images. We applied aperture correction to the magnitudes from the PSF fitting by comparing the magnitudes of isolated stars from PHOTOMETRY with those from PSF fitting.

III. RESULTS

(a) Cluster Diameter

In order to determine the center and radial extent of the cluster, we have examined the density distribution of the stars in the field of Be 2. As is seen in Fig. 1 and Fig. 2, it is not too difficult to define roughly the center of the cluster by visual inspection. However, we have determined the cluster center by plotting the stellar density distributions in x and y (pixels) with 30 pixel intervals.

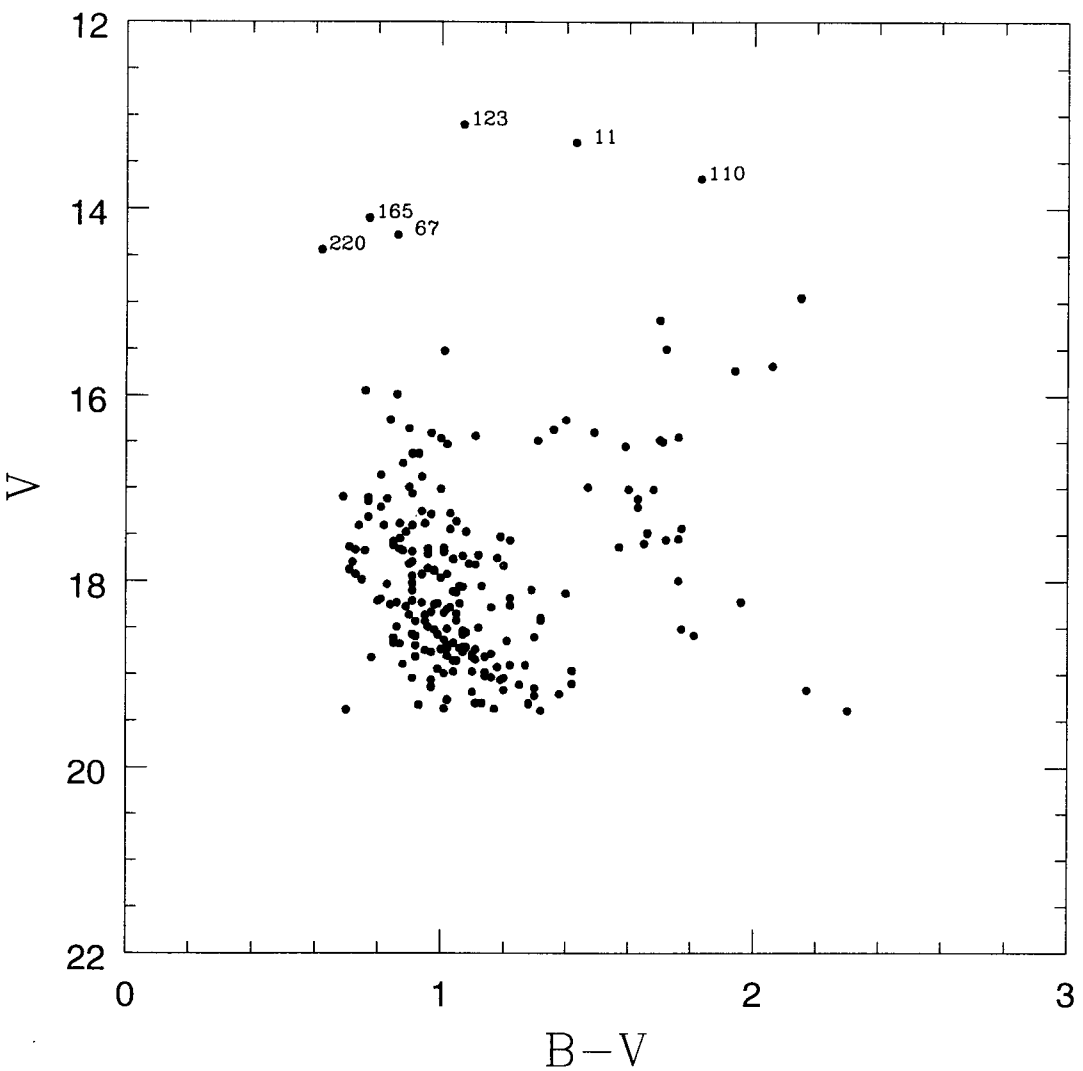

Fig. 5. CMD of Be 2. All the stars in Table 2 are plotted. The Six brightest stars are identified.

Table 2. UBV Photometry in Berkeley 2

ID	X	Y	V	$B-V$	$U-B$	ID	X	Y	V	$B-V$	$U-B$
1	2.8	93.0	16.49	1.31		49	113.3	126.7	18.05	1.06	0.82
2	3.4	79.5	19.17	1.20		50	114.5	85.5	17.44	1.03	0.69
3	10.1	159.0	19.31	1.13		51	114.5	119.9	18.57	1.07	0.42
4	14.2	195.9	15.52	1.01	0.39	52	115.7	92.0	19.04	1.20	
5	19.3	173.4	17.25	0.94	0.53	53	118.2	220.2	16.41	0.97	0.52
6	21.0	257.3	19.23	1.30		54	119.4	137.5	17.64	1.01	0.63
7	21.0	381.4	18.68	1.02		55	121.1	277.6	18.23	0.94	0.39
8	23.4	96.8	19.21	1.38		56	122.1	417.8	17.87	0.71	0.46
9	24.3	170.3	18.72	1.02		57	124.5	124.0	18.72	1.06	0.41
10	29.5	80.4	17.92	1.02	0.55	58	128.1	408.2	19.06	1.19	
11	35.7	274.9	13.29	1.43	1.14	59	133.8	226.5	19.06	0.97	
12	36.8	201.2	17.65	0.96	0.59	60	138.5	248.4	16.55	1.59	1.07
13	37.2	179.1	18.11	1.04	0.98	61	138.6	420.0	17.66	0.73	0.52
14	38.9	358.0	17.96	1.00	0.36	62	139.1	253.5	18.69	0.92	
15	42.1	295.9	18.35	1.05	0.55	63	140.4	120.7	18.90	1.27	
16	43.2	449.1	18.64	1.21		64	140.6	392.2	19.71	1.16	
17	44.5	308.9	17.40	0.74	0.71	65	144.6	44.3	18.13	1.40	
18	47.2	330.7	18.63	1.01		66	145.3	210.9	17.01	1.00	0.97
19	48.1	160.8	18.76	0.97	-0.40	67	152.9	76.9	14.28	0.86	0.22
20	51.5	367.1	17.10	0.77	0.71	68	153.5	138.3	18.80	1.02	
21	53.2	441.5	17.76	1.04	0.80	69	154.8	202.1	17.01	1.68	1.35
22	54.5	244.1	18.43	0.92	0.70	70	155.2	434.0	18.59	0.92	
23	56.0	319.0	17.81	1.09	0.82	71	156.6	225.4	17.06	0.91	0.79
24	57.0	259.1	18.92	1.18		72	158.7	88.9	17.63	1.57	
25	59.1	15.8	18.35	1.05	-0.29	73	161.3	63.2	19.15	1.30	
26	60.8	450.5	18.96	1.42		74	162.8	86.6	16.99	1.47	0.61
27	62.4	208.4	17.67	0.88	0.88	75	168.8	219.2	16.99	0.90	0.71
28	62.7	216.4	17.72	1.12	0.41	76	171.0	354.7	17.92	0.73	0.97
29	63.8	194.9	18.97	1.04		77	172.2	342.5	17.14	0.77	0.80
30	65.3	162.6	18.24	0.99	0.88	78	172.8	135.2	17.28	0.97	0.91
31	65.5	346.7	18.76	1.07		79	175.1	330.0	18.89	0.88	
32	66.2	276.4	17.54	0.87	0.68	80	180.3	132.8	18.05	1.13	0.55
33	67.9	404.8	18.21	0.80	0.40	81	180.6	271.1	18.67	0.87	
34	68.1	170.9	18.25	0.84		82	180.9	208.4	17.48	1.66	1.45
35	68.5	265.4	17.11	0.83		83	181.0	266.7	18.10	0.91	
36	68.6	71.7	18.22	1.96		84	181.1	237.2	19.31	1.28	
37	68.9	30.1	18.78	1.10	0.12	85	181.2	180.9	18.57	0.99	
38	71.7	260.9	18.03	0.83		86	182.6	281.9	18.58	1.81	
39	77.7	313.0	18.27	0.89	0.45	87	183.7	387.8	16.37	1.36	1.07
40	81.2	452.6	15.95	0.76	0.46	88	185.3	402.6	16.53	1.02	0.98
41	81.9	223.5	18.81	1.10		89	186.7	253.4	17.65	0.87	0.73
42	87.8	218.9	17.75	1.18	0.49	90	188.7	174.9	16.88	0.94	0.75
43	99.2	214.4	18.90	1.22		91	190.0	432.5	19.11	1.25	
44	99.4	252.0	18.23	0.86	0.79	92	190.2	201.9	19.02	1.14	
45	104.2	338.9	17.31	0.77	0.74	93	191.0	242.5	16.26	1.40	0.85
46	105.6	187.4	18.55	1.08	-0.12	94	191.1	324.8	17.83	1.20	1.01
47	107.5	182.2	18.26	1.22		95	191.1	231.6	18.94	0.99	
48	108.9	422.4	18.84	1.11		96	193.7	269.7	15.50	1.72	1.32

Table 2. Continued

ID	X	Y	V	$B-V$	$U-B$	ID	X	Y	V	$B-V$	$U-B$
97	195.5	303.7	17.01	1.60	0.97	145	249.8	197.2	18.73	1.00	0.21
98	196.3	132.6	17.81	0.90	0.67	146	251.6	324.1	19.13	0.97	
99	196.3	225.1	16.73	0.88	0.72	147	252.2	262.4	18.50	1.12	
100	197.3	407.1	17.09	0.69	0.63	148	254.4	208.6	15.73	1.94	1.37
101	198.0	251.5	16.63	0.91	0.66	149	255.6	321.8	17.40	0.82	0.62
102	199.2	25.6	19.37	1.01		150	256.1	249.4	18.51	1.02	
103	202.7	150.3	18.51	1.77		151	257.7	276.3	17.40	0.91	0.70
104	205.8	239.7	18.36	0.95		152	258.6	228.9	16.63	0.93	
105	206.5	327.1	19.28	1.02		153	260.6	223.5	17.68	0.91	0.66
106	206.9	192.0	17.57	0.85	0.59	154	263.5	426.1	19.39	1.32	
107	207.9	46.7	17.54	1.76		155	268.3	45.5	17.59	1.65	0.76
108	208.7	142.4	16.44	1.11	0.49	156	268.7	415.0	18.71	1.08	
109	210.0	172.7	17.43	1.77	1.26	157	268.7	85.8	16.47	1.00	0.32
110	214.6	207.2	13.68	1.83	1.23	158	269.0	193.6	17.67	1.01	1.05
111	214.8	214.8	17.20	1.63		159	269.8	401.4	18.82	0.78	0.13
112	219.1	18.4	16.45	1.76	1.06	160	270.3	372.4	17.82	1.11	
113	219.8	333.6	17.11	1.63	0.97	161	270.9	332.0	17.94	0.91	0.51
114	220.9	100.3	17.86	0.96	1.09	162	271.0	251.4	18.49	0.96	0.61
115	221.1	292.7	18.02	0.91		163	276.2	438.4	17.98	0.75	0.63
116	223.0	257.4	18.06	1.07	0.44	164	276.3	11.3	19.06	1.19	
117	224.0	7.2	16.40	1.49	0.99	165	276.5	232.1	14.10	0.77	0.26
118	224.9	295.3	16.26	0.84	0.73	166	276.6	322.0	19.32	1.28	
119	226.0	201.9	17.69	1.01	0.86	167	278.1	155.4	19.03	1.16	
120	226.9	221.7	17.93	0.94	0.74	168	278.9	312.5	18.42	1.05	0.24
121	228.1	196.5	18.24	1.06		169	279.6	352.8	19.27	1.02	
122	228.8	145.2	16.50	1.71	0.82	170	280.1	83.7	18.39	1.32	
123	231.4	171.2	13.10	1.07		171	282.3	126.4	17.71	0.96	0.73
124	231.7	262.2	18.53	1.07		172	282.8	217.7	18.78	1.16	
125	231.8	23.8	17.79	0.91	0.67	173	283.1	62.7	17.99	1.76	
126	233.0	256.9	18.30	1.02		174	286.1	325.1	18.42	1.32	
127	233.0	346.3	15.99	0.86	0.34	175	290.8	252.3	19.37	1.17	
128	233.9	59.0	14.95	2.15	1.38	176	291.6	300.6	18.52	0.98	
129	234.7	217.6	17.47	1.08	0.87	177	292.2	150.4	18.25	0.98	1.13
130	236.8	287.7	18.19	0.81	0.55	178	293.0	29.6	19.10	1.42	
131	237.0	95.6	18.69	1.02		179	296.9	19.6	19.14	0.97	
132	238.0	389.2	10.52	0.77	0.52	180	299.0	297.2	18.57	0.91	
133	238.3	71.2	18.81	1.14		181	299.2	267.5	18.09	1.29	
134	238.9	448.3	19.33	0.93		182	304.8	211.4	17.55	1.72	
135	239.7	229.9	16.36	0.90	0.77	183	308.6	253.8	17.88	0.98	0.57
136	239.7	217.1	19.04	0.91		184	308.5	356.0	17.20	0.81	0.81
137	239.7	277.8	17.73	1.07	0.33	185	312.7	411.5	17.63	0.71	0.67
138	241.8	128.8	19.19	1.10		186	314.8	171.9	15.68	2.06	
139	245.0	418.7	17.79	0.72		187	315.8	103.1	17.89	0.98	0.44
140	245.4	183.2	17.27	1.03	0.82	188	321.0	330.8	18.81	0.92	
141	246.1	93.1	17.56	1.22	0.57	189	321.7	381.8	18.49	0.86	0.51
142	246.4	216.3	18.33	0.97	0.66	190	323.2	367.7	17.67	0.76	0.60
143	247.5	264.7	17.61	0.85	0.43	191	324.0	242.7	18.12	1.05	
144	248.0	347.4	16.86	0.81	0.76	192	324.2	103.2	18.60	1.30	

Table 2. Continued

ID	X	Y	V	$B-V$	$U-B$	ID	X	Y	V	$B-V$	$U-B$
193	324.6	271.6	18.21	0.91		209	349.6	98.9	19.31	1.11	
194	324.9	375.0	18.99	1.01		210	350.0	296.9	18.61	0.85	-0.05
195	330.9	152.1	18.85	1.04		211	354.5	200.6	17.38	0.95	0.34
196	331.6	137.7	19.39	2.30		212	355.9	154.5	18.28	1.16	
197	331.6	316.9	18.36	0.90	0.65	213	356.2	28.0	19.17	2.17	
198	334.5	13.3	18.66	0.85		214	359.5	378.2	17.38	0.87	0.23
199	336.8	344.0	18.34	1.01		215	365.2	327.9	15.19	1.70	1.23
200	337.1	83.1	18.43	0.95		216	365.4	39.8	18.18	1.22	
201	337.6	383.9	19.38	0.70		217	365.4	212.0	18.74	0.95	
202	338.0	198.5	18.66	1.04	0.08	218	370.4	75.9	17.36	1.05	0.76
203	340.7	389.4	18.98	1.14		219	371.9	31.3	16.48	1.70	1.07
204	343.5	236.9	17.47	0.89		220	375.7	377.6	14.44	0.62	0.39
205	343.9	290.0	18.71	1.07		221	378.1	236.7	17.52	1.19	0.50
206	347.2	337.8	18.85	1.05		222	381.8	149.4	18.97	1.10	
207	348.1	352.4	18.73	1.11		223	383.1	346.1	18.28	1.03	0.62
208	349.0	231.8	17.92	0.94	0.58						

Because the region covered by CCD frame is not large enough to derive the density distribution far outside the cluster, we used the DSS image of $10' \times 10'$, centered on the Be 2, as well as our CCD images to analyze the radial extent of Be 2. Fig. 4 shows the stellar surface density distribution as a function of distance from the cluster center. The left panel shows the density distribution from the CCD image and the right panel is that for the DSS image. The surface density decreases outward until $r \sim 130''$ with a change in slope at $r \sim 90''$ and flattens beyond $r \sim 130''$, which suggests the boundary of the cluster lies near $r \sim 130''$. Therefore, it is reasonable to take the diameter of the cluster as $260''$ which is more than two times larger than the diameter given in COCD.

(b) The Color-Magnitude Diagram

To our knowledge, this study is the first photometric study of Be 2. Fig. 5 shows the CMD of the stars in the field of Be 2. We plotted all the stars listed in Table 2. Because our CCD frame covers most of the cluster field, the CMD in Fig. 5 includes most of the cluster member stars which are brighter than $V \sim 19.4$. Despite the presence of many field stars both on the right and on the left of the main sequence in the CMD of Be 2, the cluster sequence is well visible.

The main sequence of the cluster is quite broad due to the large photometric errors in $(B-V)$ colors. Most of the stars located on the right of the cluster sequence are thought to be field giants. However, it is quite probable that some of them, especially brighter ones, are cluster members. Presence of six brightest stars marked by the identification number of Table 2 is a puzzle in the CMD. They are much brighter ($\Delta m \geq 2$) than the turnoff. As is seen in Fig. 2, the spatial distribution of these stars implies that some of them might be cluster members. But the large gap in the main sequence suggests that they are probably forground stars.

(c) Reddening and Distance

We have plotted apparent *(U-B)* versus *(B-V)* diagram for the stars within $1'$ from the cluster center with photometric errors in *B-V* colors less than 0.1 mag to determine the reddening to the cluster. The stars in the central part of the cluster are less contaminated by the field stars, and thus better estimate of the reddening to the cluster is possible for these stars. We performed the color-color fit by shifting the fiducial ZAMS of Mermilliod (1981) along the reddening line with a slope of $E(B-V)/E(U-B) = 0.72$ (Johnson & Morgan 1953) which is represented as a continuous straight line in the upper right part of the diagram. Due to large photometric errors in $(U-B)$ colors, it is impossible to estimate the reddening value precisely. However, it was found that the reddening to the cluster lies between 0.7 and 0.9. Among these values, the reddening value which gives the best fit of the isochrones to the stellar distributions in the CMD of Be 2 is $E(B-V) = 0.80 \pm 0.05$.

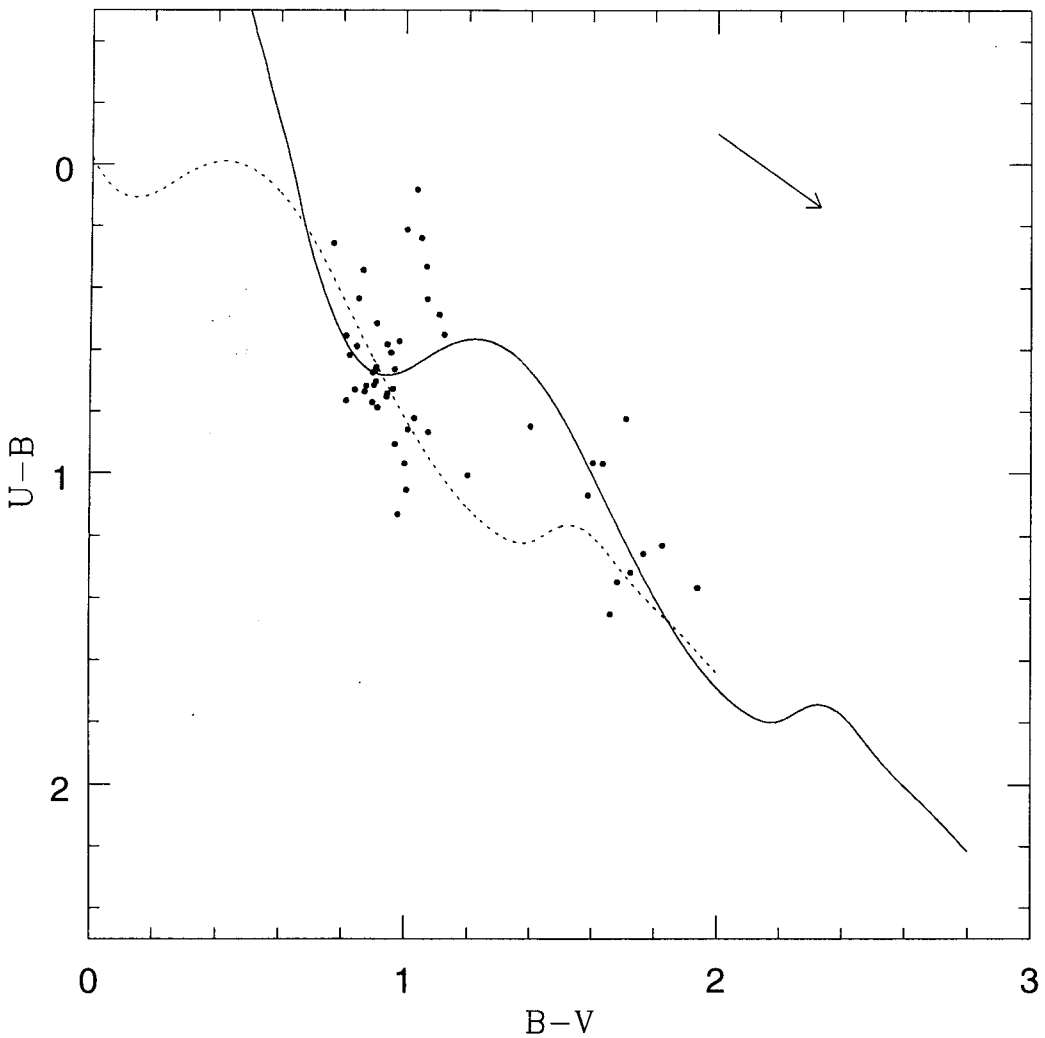

Fig. 6. Color-color diagram of Be 2. The stars within 1′ from the cluster center with photometric errors in B-V colors less than 0.1 mag are plotted. The dotted line is the fiducial ZAMS of Mermilliod and the solid line is that shifted along the reddening line by $E(B\text{-}V) = 0.80$.

Because our photometry did not reach to the main sequence far below the turnoff, we have obtained a rough estimate of the distance modulus, $(m - M)_o = 13.5 \pm 0.5$, by shifting the fiducial ZAMS (Mermilliod 1981) in the $V-(B-V)$ CMD after the reddening to the cluster was determined. This estimate of the distance modulus was used as a constraint in the isochrone fitting to the observed CMD in the next section. We have used the total-to-selective absorption ratio, R=3.0 for the interstellar absorption correction in the distance estimate.

(d) Isochrone Fitting and Cluster Parameters

We have applied isochrone fitting to the observed CMD of Be 2 to determine reddening, distance modulus, age and metallicity, simultaneously, using the Padova isochrones (Bertelli *et al.* 1994) that were available at the Starsbourg Data center. Evolution tracks of Padova group cover mass range of $(0.5 \sim 120)\,M_\odot$ and reach the tip of the asymptotic giant branch or the ignition of the core C-O burning phase, depending on the initial stellar mass. They take into account the possible overshooting from convective cores.

The age of Be 2 is estimated to be $\sim$ 800 Myr from the isochrone fitting to the observed stellar distribution in CMD. We used only the photometry of the stars in the central part of Be 2 ($r \leq 1'$) with photometric errors less than 0.1 mag in V and brighter than $V \sim 19.4$. As is seen in Fig. 7, the isochrones of log (t) = 8.8, 8.9 and 9.0

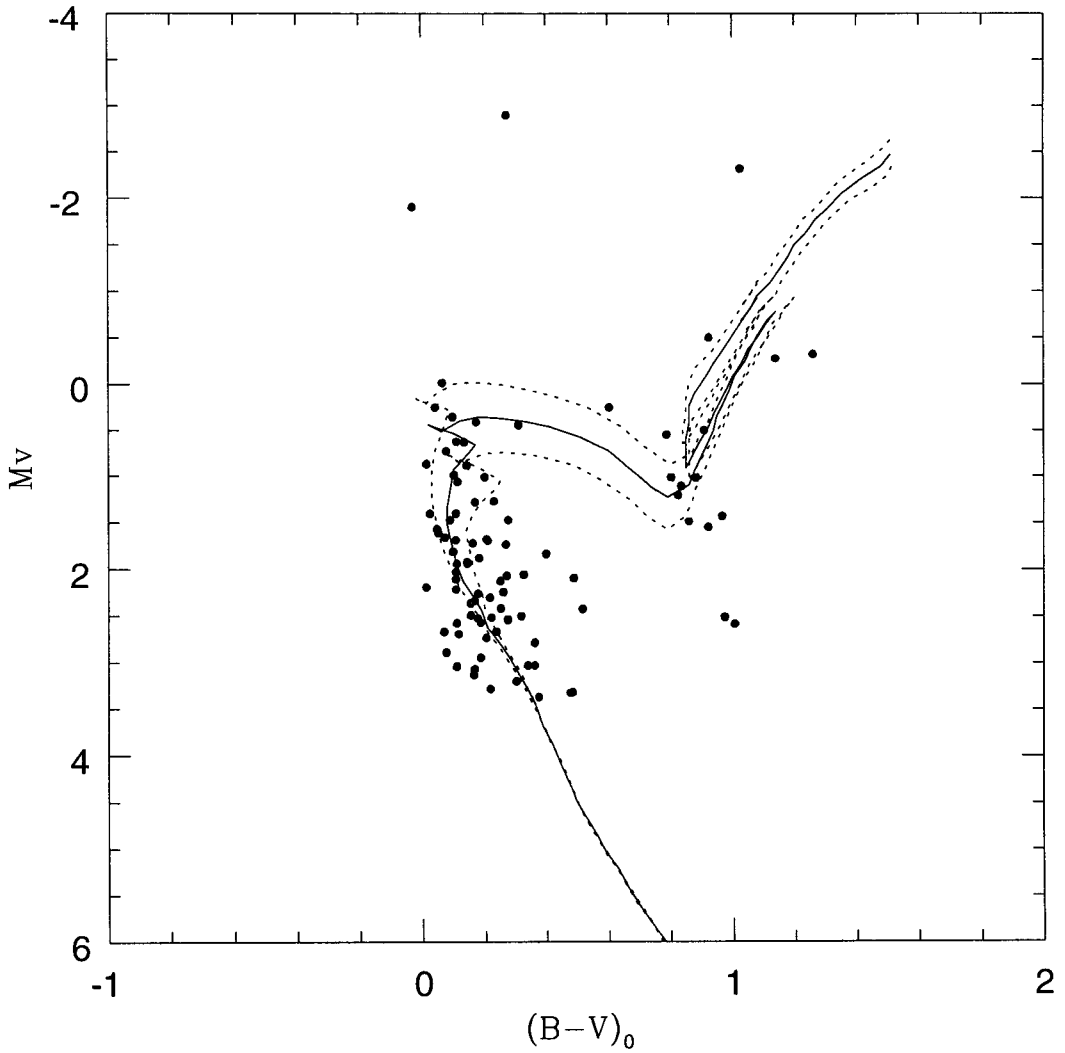

Fig. 7. CMD of the satrs in the central part ($r \leq 1'$) of Be 2. The Padova isochrones of log (t) = 8.8, 8.9 and 9.0 with Z = 0.008 are overlaped with the assumption of $E(B\text{-}V)$=0.80 and $(m\text{-}M)_o$=13.6.

with Z = 0.008 seem to fit well the stellar distribution near the turnoff point as well as the giant branch and the lower main sequence.

Here the reddening of $E(B-V)$=0.80 and true distance modulus of $(m-M)_o$ = 13.6, which corresponds to 5.2 kpc from the Sun, were adopted, respectively. We neglected the three brightest stars in Fig. 7 in the isochrone fitting because they are probably field stars.

IV. DISCUSSION

An accurate determination of the reddening and distance to the cluster is essential to understand the physical properties of open clusters. The main sequence fitting method which has been applied to the present photometry is a straight forward one to estimate the reddening and distance of open clusters. However, it is not so simple to fit the fiducial ZAMS to the observed stellar distributions in the color-color diagrams and CMDs, because these diagrams are contaminated by field stars.

The most common practice of field star discriminaton is to use membership probabilities of the stars in the cluster

field, based on proper motion study and/or radial velocity data. Spectral classification also seems to be useful for discriminating the field stars from the CMDs of open clusters (Sears & Sowell 1997). In the case of Be 2, there is virtually no way to distinguish the cluster stars from the background/foreground stars due to lack of kinematic informations and spectral types, even for the brighter stars. However, the present estimates of the reddening and distance to the cluster by main sequence fittings are not much affected by the field stars because most of the bright stars in the central part of the cluster ($r \leq 1'$) are thought to be cluster members. The good agreement between the reddening and distance to the cluster determined by the main sequence fittings and those from isochrone fitting strongly indicates that the present estimates of the reddening and distance of Be 2 are reasonable.

The isochrone fitting is a trial-and-error task of fitting four parameters (distance, reddening, age and metallicity) simultaneously. The range of parameter space can be narrowed by physical constraints imposed by the characteristics of open clusters as well as the observed morphology of the photometric diagrams. We excluded the extremely young and old isochrones in the isochrone fitting because the morphology of the observed CMD of Be 2 implies an intermediate age for Be 2. We also excluded the isochrones of extreme metallicities in the isochrone fitting. The metallicity of Be 2 derived from the isochrone fittings to the observed stellar distribution in CMD is consistent with that inferred from the metallicity gradient of the Galactic disk (Friel & Janes 1993) at the position of Be 2.

V. SUMMARY

We have presented *UBV* CCD photometry of an unstudied open cluster Be 2. Our photometry covers a field of $3.'2 \times 3.'8$ of the sky centered on the cluster. The radial extent of Be 2 is found to be $\sim 260''$ in diameter which is about two times larger than the diameter given in COCD. Due to large photometric errors in $U-B$ colors and lack of photometry for lower main sequence stars, only rough estimates of the reddening and distance to the cluster were possible by main sequence fittings. But these values were useful to constrain the reddening and distance in simultaneous determination of the four cluster parameters (reddening, distance, age and metallicity) by isochrone fitting. We have used the theoretical isochrones from Padova evolutionary tracks which take into account the overshooting from convective cores.

The best fit of isochrones to the observed CMD has been achieved by the isochrones of $log(t) = 8.9 \pm 0.1$ with heavy element abundance Z = 0.008, with the assumption of reddening and distance modulus as $E(B-V) = 0.8 \pm 0.05$ and $(m-M)_o = 13.6 \pm 0.1$, respectively. The resulting age of $\sim 800 Myr$ is consistent with the morphology of the cluster which resembles that of the intermediate-age open clusters. The metallicity of Be 2 from isochrone fitting is consistent with that inferred from the metallicity gradient of the Galactic disk at the position of Be 2.

ACKNOWLEDGEMENTS

We thank Myung Gyoon Lee and Hwankyung Sung for critical reading of an earlier version of the manuscript and useful comments. This work was supported in part by the KOSEF Grant through Grant No 95-0702-01-01-3.

REFERENCES

Bertelli, G., Bressan, A., Chiosi, C., Fagotto, F., & Nasi, E. 1994, A&AS, 106, 275
Christian, C. A., Adams, M., Barnes, J. V., Hayes, D. S., Siegel, M., Butcher, H., & Mould, J. R. 1985, PASP, 97, 363
Friel, E. D., & Janes, K. A. 1993, A&AS, 267, 75
Johnson, H. L., & Morgan, W. W., 1953, ApJ, 117, 313
Kaluzny, J. 1994, A&AS, 108, 151
Lyngå, G. 1987, Catalog of Open Cluster Data, Starsbourg, Centre de Donnees Stellaires. 5th ed.
Massey, P., & Davis, L. E., 1992, A User's Guide to Stellar Photometry with IRAF
Mermilliod, J. C. 1981, A&A, 97, 235
Phelps, R. L., & Janes, K. A. 1994, ApJS, 90, 31
Phelps, R. L., Janes, K. A., & Montgomery, K. A. 1994, AJ107, 1079
Sandage, A. 1955, ApJ, 128, 150
Sears, R. L., & Sowell, J. R. 1997, AJ, 113, 1039